Transactions of the Materials Research Society of Japan 27 [2] 313-316 (2002)

Two-Dimensional Simulation of Microstructural Changes during Superplastic Deformation

Byung-Nam Kim and Keijiro Hiraga
National Institute for Materials Science, 1-2-1 Sengen, Tsukuba, Ibaraki 305-0047, Japan
Fax: 81-298-59-2501, e-mail: KIM.Byung-Nam@nims.go.jp

Superplastic deformation accompanied by static grain growth is simulated in two-dimensional polycrystalline solids on the basis of a mantle model, where a soft zone called mantle is formed along grain boundaries by grain boudnary sliding, and where diffusion along the mantle controls the macroscopic deformation. The microstructural features during deformation are found to be different from those during static grain growth, and are characterized by the broader distribution of the number of sides. The simulated microstructural evolution also shows the characteristics of active grain boundary sliding and increasing grain aspect ratio with strain. It is noticeable that grain boundary sliding contributes considerably to the superplastic deformation even for highly elongated microstructures.
Key words: grain boundary, diffusion, mantle, aspect ratio, strain

1. INTRODUCTION

Recently, we conducted the simulation of high-temperature deformation accompanied by both static and dynamic grain growths in two-dimensional (2D) polycrystalline solids [1]. The simulation is based on the mechanism of grain boundary diffusion, and predicted the relationship between microstructural changes and mechanical responses for varying grain boundary mobilities. According to the simulation, for zero grain boundary mobility, the grain aspect ratio during the deformation can be obtained directly from the grain strain, which means that the grain strain corresponds to the macroscopic strain. With increasing grain boundary mobilities, the increasing rate of the grain aspect ratio with strain becomes lower. For superplastic deformation, however, the experimentally observed relationships between the grain aspect ratio and the macroscopic strain have much lower increasing rate than the ones obtained by the simulation even for high grain boundary mobilities. Hence, the actual microstructural changes during superplastic deformation, where active grain boundary sliding occurs, could not be reproduced by the simulation. In the present study, we develop the algorithm for simulating superplastic deformation of 2D polycrystalline solids, which mechanism is deeply related to grain boundary sliding (GBS).

2. MICROSTRUCTURAL SIMULATION

2.1 A mantle model

When two grains are slided by a shear strain of γ, the strain is concentrated around grain boundary, and grain interior far from the boundary remains rigid. According to the atomistic simulation of GBS by Molteni et al. [2], bond-breaking spreads away from the boundary, and a zone of disordered atomic structure is formed around the boundary. This means that the strain decreases to zero gradually with increasing distance from the boundary. For infinitesimal γ, the deformation is elastic, and above the elastic limit, the atomic structure around the boundary becomes unstable, providing that dislocation activity is limited. The unstable structure is assumed to be amorphous in this study.

The GBS with the amorphous region is similar to the problem of shear of two rigid plates sandwiching a ductile matrix (mantle). Such shear deformation can be described by introducing the concept of geometrically-necessary dislocations. According to Ashby [3], the average density of geometrically-necessary dislocations ρ in the deformed mantle is represented by $2\gamma/(bd)$, where b is the Burgers vector and d is the mantle width. ρ and d increase with increasing γ. In the dislocation density, however, there is a limit value available in the material, and the atomic structure with the limit density is often considered to be amorphous. Hence, the dislocation density in the amorphous mantle can be represented by the limit value ρ^*.

If additional strain is not supplied, the excited atomic structure in the mantle will be relaxed and return to the original crystalline state. In contrast, at steady state of GBS, d is constant and obtained by $c_1\dot{\gamma}t_c/(b\rho^*)$, where c_1 is a constant, $\dot{\gamma}$ is the shear strain rate and t_c is the characteristic time for the structure-relaxation. Providing that the amorphous mantle is viscous, d becomes $c_1 t_c \tau/(b\rho^* \eta)$, where τ is the shear stress and η is the viscosity. The mantle appears proportional to the shear stress at steady state.

In polycrystals subjected to uniaxial tension, the component of shear stress on grain boundary depends on the boundary angle with respect to the tensile axis. The rate of GBS, however, is not dependent solely on the shear stress component, because all GBSs are interrelated for maintaining microstructural coherency. The actual GBS behavior in polycrystals is quite complex. Hence, we assume that at steady state deformation, d is uniform at all grain boundaries in polycrystals.

When diffusion occurs along the amorphous mantle, its contribution to deformation is considerable compared to that of grain boundary diffusion due to the wider path and high diffusivity. Since the atomic structure in the amorphous mantle is excited as in grain boundary, the diffusivity is expected to be nearly identical to that in grain boundary. Hence, at high stresses where the mantle is formed of sufficient width, the deformation mechanism can be changed to mantle diffusion from grain boundary diffusion.

The deformation mechanism of mantle diffusion is very similar to that of grain boundary diffusion, so that we can modify the constitutive equation for grain boundary diffusion. For the deformation by grain boundary diffusion,

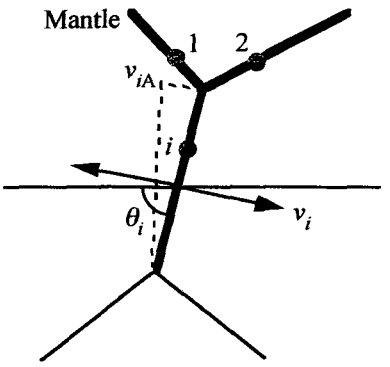

Fig. 1 Grain boundary mantle as a computing unit.

Coble [4] obtained the strain rate $\dot{\varepsilon}$ by $c_2 D_b \delta \Omega \sigma/(kTR^3)$, where c_2 is a constant, D_b is the grain boundary diffusivity, δ is the grain boundary width, Ω is the atomic volume, k and T have their usual meanings and R is the average grain radius. Replacing δ by d, we obtain

$$\dot{\varepsilon} = c_3 \frac{D_b \delta \sigma_n^2}{R^3} \tag{1}$$

where c_3 is a constant and σ_n is the normal stress of $\Omega\sigma/kT$. In this equation, d has been changed to σ_n by letting $c_2 d/\delta = c_3 \sigma_n$. Eq. (1) indicates a stress exponent of 3 and a grain size exponent of 2.

2.1 Computing algorithm

The entire structure of the present computing algorithm is similar to that in the previous simulation for diffusional creep [1]. In the following, we describe the algorithm in brief. The other details are described elsewhere [1].

First, we formulate the relative velocity of two mantle surfaces between mantle and rigid grains, caused by diffusional flux in the mantle. When the tensile stress σ is applied to mantle i making an angle of θ_i with respect to the stress axis, the chemical potential in the mantle changes by $\Omega\sigma\cos^2\theta_i$. The chemical potential is different between mantles, and the difference causes a diffusional flux between them. The diffusional flux in mantle i occurs through two ends of the mantle facet; triple points A and B. Here, we divide the diffusion process into two units. Each unit contains one triple point, as described in Fig. 1.

Consider the diffusion through triple point A. If the diffused matter is assumed to be distributed linearly along the mantle facet from 0 at the opposite triple point B, the relative velocity v_{iA} of mantle i at triple point A is obtained by

$$v_{iA} = \frac{c_4 D_b \delta \sigma_n^2}{l_i} \sum_j^2 \frac{(\cos^2\theta_i - \cos^2\theta_j)}{(l_i + l_j)/3} \tag{2}$$

where c_4 is a constant and l_i is the length of mantle i. In this equation, d has been changed to σ_n by letting $2d/\delta = c_4\sigma_n$. Although the relative velocity is varied along the mantle facet just after the diffusion, the average relative velocity v_i of mantle i can be obtained by $(v_{iA}+v_{iB})/2$.

Once the relative velocities are known at all grain boundary mantles, the macroscopic strain rate $\dot{\varepsilon}$ can be calculated by integrating the respective contributions to deformation, as in the previous simulation [1]. The translational velocities of respective rigid grains are determined by $\dot{\varepsilon}$, under an assumption of macroscopically uniform deformation.

The polycrystalline structure is deformed by increasing strain stepwise, and the positions of triple points at each step are determined in the following way. Before deformation, we determine the positions of three corners of rigid grains, which have the same distance from the triple point in a direction to the gravitational centers of respective grains. Since the translational velocities of the grain corners are identical to those of the rigid grains, they are obtained by the above uniform deformation. After stepwise deformation, a new triple point is determined to be located at the same distance from the three grain corners. Then, we can construct the deformed microstructure by connecting the triple points with straight grain boundaries.

The initial microstructure for the simulation was obtained by growing statically the Voronoi microstructure composed of 6000 grains under periodic boundary conditions. The static grain growth reached steady state when the microstructure consisted of 3300 equiaxed grains with an average grain size of about 1.5 times the initial size [5]. This microstructure is used as the initial one for the superplastic simulation. The theoretical kinetics of static grain growth at steady state can be represented by

$$\left(\frac{R}{R_0}\right)^2 - 1 = \frac{\alpha}{3} M_n t_n \tag{3}$$

where R_0 is the initial value of R, α is the geometric factor,

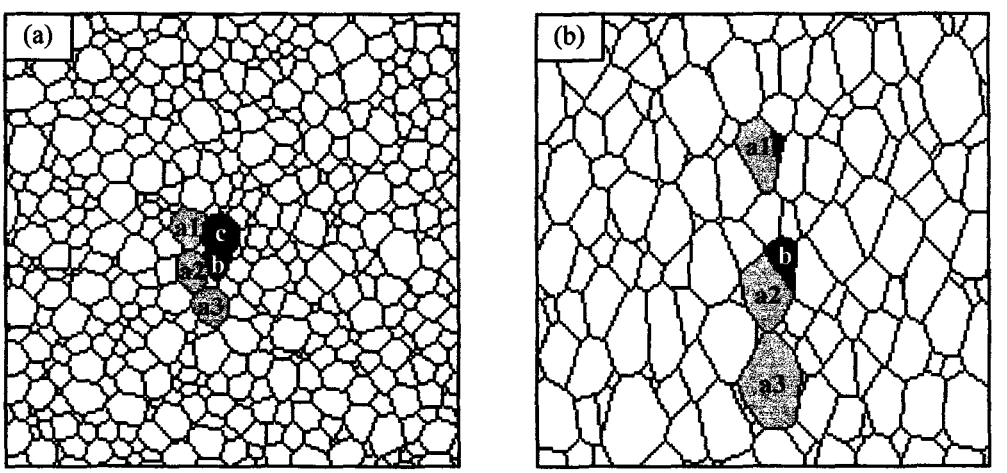

Fig. 2 Microstructural evolution for σ_n=0.4 and M_n=0.105: (a) ε=0.0 and (b) ε=1.067. The stress axis is vertical.

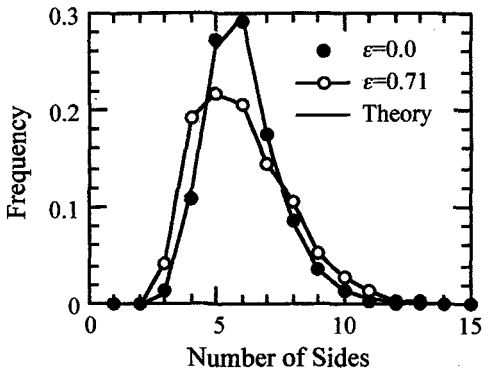

Fig. 3 Distribution of the number of sides.

and M_n and t_n are the normalized grain boundary mobility and time, respectively.

To simulate the superplastic deformation accompanied by static grain growth and the resultant microstructural changes, we regard that the static grain growth and the superplastic deformation work simultaneously and independently for infinitesimal time. Repeating the two processes, we can obtain largely deformed polycrystalline microstructure. The simulation is carried out for various grain boundary mobilities under constant stress loading.

3. RESULTS AND DISCUSSION

3.1 Microstructural evolution

Fig. 2 shows an example of the microstructural evolution. With increasing strain, grain growth, grain elongation and GBS proceed concurrently. Particularly, GBS is remarkable compared with the previous simulation for diffusional creep [1]. While GBS in the diffusional creep appeared by the shrinkage and annihilation of grains, in the present superplastic deformation, it appears by the relative displacement of grains. The reference grains (a series of 'a') in Fig. 2 show the separation behavior between them along the stress axis, which indicates the occurrence of active GBS. The role of GBS in the deformation is discussed later.

In the simulated microstructural evolution, the grain growth behavior is found to be unnormal. For normal grain growth which occurs by the curvature-driven migration of grain boundary, grains with larger number of sides than 6 grow, while those with smaller number of sides shrink. For example, grain b with 8 number of sides at the initial state of Fig. 2(a) grows in normal grain growth. However, it shrinks during the deformation. In addition, grain c which is smaller than grain b at the initial state grows to be larger at ε>1.0. Such unnormal grain growth behavior during the deformation can also be confirmed by the deviation from the normal distribution of the number of sides, as shown in Fig. 3. While the normal distribution at the initial state consists well with the theoretical prediction by Carnal and Mocellin [6], the distribution during the deformation deviates largely from the normal distribution.

Since the phenomenon of grain switching changes the number of sides for the related grains, such unexpected growth behavior of grain c can occur with a low probability. However, we consider that the unnormal grain growth is due to the perturbed grain growth mechanism. In the present simulation, the position of triple point after deformation was influenced largely by the presence of mantle at grain boundaries as well as by the normal static growth. In addition, superplastic deformation changes the grain boundary structure to be elongated. We consider that these processes perturbed the normal grain growth mechanism and resulted in the unnormal grain growth during the deformation.

3.2 Grain elongation

Despite the microstructural adjustment for retaining the equiaxed shape of grains, grain elongation increases with increasing strain, as shown in Fig. 2. The variation of the grain aspect ratio r_g with strain is shown in Fig. 4. The effects of the stress and the grain boundary mobility on the grain aspect ratio are similar to the case of the previous simulation for diffusional creep [1]. For high stresses and/or low grain boundary mobilities, the rate of grain elongation increases. The grain elongation is explained from the balance between the stress-directed diffusion along the mantle and the rearrangement of triple points during grain growth, both of which evolve the size and shape of grains. High stresses accelerate diffusion in the direction along the stress axis and low mobilities restrict the rearrangement of triple points, resulting in the enhanced grain elongation.

For low stresses and/or high mobilities, however, the restriction of the rearrangement is decreased, and accordingly grain elongation is tend to be suppressed. Under the loading condition of constant stress, as in Fig. 4, there appears a trend of decreasing aspect ratio at large strains. As a result, low stresses and/or high mobilities result in more equiaxed microstructure after deformation.

3.3 Grain boundary sliding

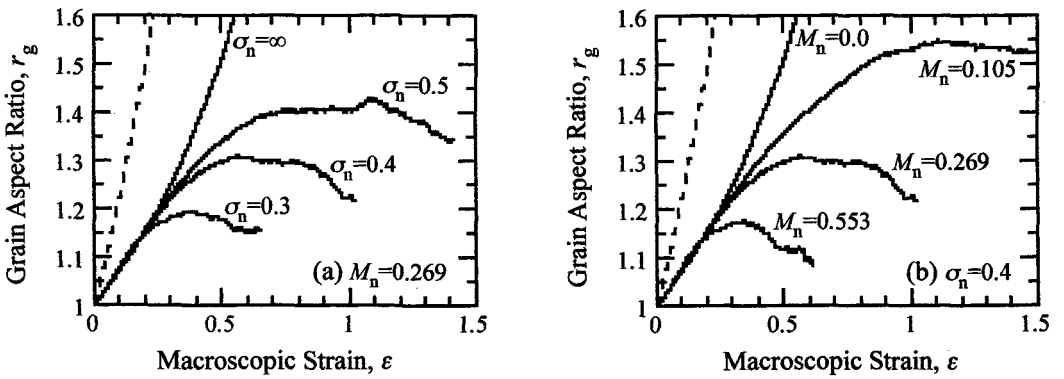

Fig. 4 Variation of the grain aspect ratio at constant stress loading: (a) for various stress levels at M_n=0.269 and (b) for various grain boundary mobilities at σ_n=0.4. The dotted curve represents the grain strain for M_n=0 in the diffusional creep.

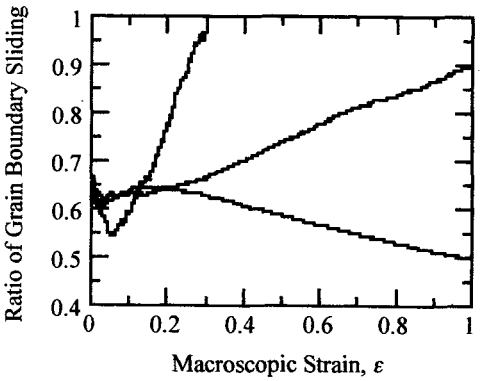

Fig. 5 Variation of the ratio r_s of the GBS strain to the macroscopic strain.

As shown in Fig. 4, the rate of grain elongation in the superplastic deformation is lower than that in the diffusional creep. Comparing r_g for the two cases of M_n=0 in Fig. 4(b), the increasing rate of r_g in the superplastic deformation is less than half the rate in the diffusional creep. Since the macroscopic strain corresponds to the grain strain in the diffusional creep for M_n=0, the lower increasing rate of r_g in the superplastic deformation indicates that GBS contributes to the macroscopic strain.

GBS can be classified into two types [7]. One is Lifshitz GBS which accommodates stress-directed diffusion, and the other is Rachinger GBS which displaces grains with respect to each other by retaining essentially their original shape. Lifshitz GBS contributes to the axial strain, but the contribution is included in the grain strain, so that the macroscopic strain in the previous simulation corresponded to the grain strain for M_n=0. The slight GBS observed in the previous simulation [1] is a result of the Lifshitz GBS. Most GBSs observed during superplastic deformation is a Rachinger type. Rachinger GBS has been considered to contribute to the total strain along with the grain strain, and is regarded as a primary deformation mechanism in superplastic deformation. Hence, the active GBS observed in Fig. 2 can be defined as a Rachinger type.

When the macroscopic strain during superplastic deformation is represented by a sum of the grain strain and the (Rachinger) GBS strain, the GBS strain can be obtained simply by subtracting the grain strain from the macroscopic one. Fig. 5 shows the variation of the ratio r_s of the GBS strain to the macroscopic strain during the deformation at constant stress loading. At ε>0.15, the ratio r_s for M_n=0 decreases with increasing ε, while it increases for M_n=0.269. This results from the varying grain aspect ratio during the deformation. For M_n=0, the grain aspect ratio r_g increases with strain to be 2.72 at ε=1, so that it becomes difficult for GBS to occur due to the extending diffusion distance, which causes the decreasing r_s. It is should be noted, however, that the contribution of grain boundary sliding to the superplastic deformation is still considerable even for the highly elongated microstructures. For M_n>0, the migration of grain boundary reduces r_g and assists GBS to occur, which causes the increasing r_s.

On the other hand, r_s shows a transition behavior at the initial state of the deformation, as shown in Fig. 5. The case of M_n=0 is typical, where the initial r_s represents relatively large variation. This is because of the transition of the microstructure from static to dynamic steady state. As shown in Fig. 3, the microstructural characteristics during deformation are different from those during static grain growth. The static microstructure which is stable before deformation changes to the dynamic one which is stable during deformation. Hence, the transition behavior of r_s appears at the initial state of the deformation. Extrapolating the curve for M_n=0 to ε=0, we obtain the r_s-value of about 0.7 for the equiaxed microstructure (r_g=1).

4. SUMMARY AND CONCLUSIONS

We made a mantle model for superplastic deformation, where a soft zone of disordered atomic structure is formed along sliding grain boundaries. The mantle is formed proportional to the sliding rate or the applied stress, and is assumed to have uniform width at all grain boundaries in polycrystals. When diffusion along the mantle controls the deformation of the polycrystals, a stress exponent of 2 and a grain size exponent of 3 are obtained from the model.

Based on the mantle model, we developed a computing algorithm for simulating microstructural evolution during superplastic deformation of 2D polycrystals composed of flat grain boundaries. The simulation was performed under constant stress loading by taking the effect of static grain growth into account, and revealed the following characteristic features of superplasticity.

1. The microstructural characteristics at steady state during deformation are different from those during annealing alone. The distribution of the number of sides during deformation are broader than that during static grain growth. A transition behavior from static to dynamic steady state occurs at the initial state of deformation.
2. Grain elongation is controlled by the balance between the grain boundary mobility and the rate of stress-directed diffusion. The grain elongation is enhanced for high stresses and low mobilities, while it is suppressed for low stresses and high mobilities.
3. Active grain boundary sliding is found to occur in the present simulation of superplastic deformation. The ratio of the strain by grain boundary sliding to the macroscopic strain decreases with increasing grain aspect ratio; from 0.7 for equiaxed grains to 0.5 for r_g=2.72. It is noticeable that grain boundary sliding contributes considerably to the superplastic deformation even for highly elongated microstructures.

5. REFERENCES

[1] B. -N. Kim and K. Hiraga, *Acta Mater.*, 48, 4151-59 (2000).
[2] C. Molteni, G. P. Francis, M. C. Payne and V. Heine, *Phys. Rev. Let.*, 76, 1284-87 (1996).
[3] M. F. Ashby, *Phil. Mag.*, 21, 399-424 (1970).
[4] R. L. Coble, *J. Appl. Phys.*, 34, 1679-82 (1963).
[5] B. -N. Kim, *Mater. Sci. Eng.*, A283, 164-71 (2000).
[6] E. Carnal and A. Mocellin, *Acta. Metall.*, 29, 135-43 (1981).
[7] W. R. Cannon, *Phil. Mag.*, 25, 1489-97 (1972).

(Received December 30, 2002; Accepted April 30, 2002)